

## Electronic Supplementary Information

### More Is Better: Aggregation Induced Luminescence and Exceptional Chirality and Circularly Polarized Luminescence of Chiral Gold Clusters

Xiao-Yan Wang,<sup>+a</sup> Jing Zhang,<sup>+ab</sup> Jun Yin,<sup>a</sup> Sheng Hua Liu<sup>\*a</sup> and Ben Zhong Tang<sup>\*b</sup>

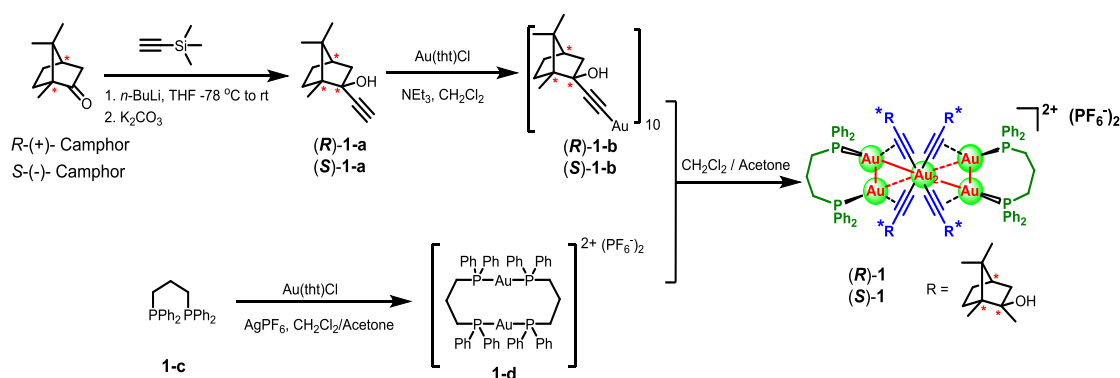
#### Measurements and Materials

NMR spectra were measured using Bruker AVANCE III HD-400 instrument. Mass spectra were measured on a Bruker micrOTOF 10223 instrument in the ESI+ mode. PL spectra were obtained by Edinburgh FLS1000 spectrometer with Xe lamp as excitation light source or an Ocean Optics QEpro spectrometer. Decay curves and were measured by Edinburgh FLS1000 spectrometer with  $\mu$ F2 lamp as excitation light source. Absolute quantum yields were achieved on FLS1000 spectrometer equipped with a calibrated integrating sphere from Edinburgh Instruments. The X-ray crystal-structure data were obtained by the Bruker APEX DUO CCD system. Circular dichroism (CD) spectra were recorded with a Chirascan spectrometer (Applied Photophysics, England). Circularly polarized photoluminescence (CPPL) spectra were recorded at 50 nm min<sup>-1</sup> scan speed with a commercialized instrument JASCO CPL-300 at room temperature with the resolution of 15 nm. Characterizations morphological structures of the aggregates were investigated by a HITACHI-SU8010 scanning electron microscope (SEM) at accelerating voltages of 200 and 5 kV, respectively.

All manipulations were carried out in argon atmosphere by using standard Schlenk techniques. *R*-(+)- and *S*-(-)- Camphor were purchased from Aladdin Industrial Corporation and used without further purification. 1,3-Bis(diphenylphosphino)propane (**1-c**) was purchased from Xin Shen Shi Hua Gong Company (China) and used without further purification. Au(tht)Cl (tht = tetrahydrothiophene) was synthesized according to published procedures.<sup>1</sup> All solvents were dehydrated and degassed before use.

## Computational Details

DFT calculations were performed with the Gaussian 09 program,<sup>2</sup> at the wb97x/6-31G\* levels of theory. Geometry optimizations were performed without any symmetry constraints. Electronic transitions were calculated by the time-dependent DFT (TD-DFT) method. The MO contributions were generated using the Multiwfn2.6.1\_bin\_Win package<sup>3</sup> and plotted using GaussView 6.0. The solvation effects in THF are included for a part of the calculations with the conductor-like polarizable continuum model (CPCM).



**Scheme S1** Synthetic route of (**R**)-1 and (**S**)-1 (tht = tetrahydrothiophene).

Synthesis of (**R**)- and (**S**)-1-a: (**R**)-1-a and (**S**)-1-a were synthesized according to the literature procedure.<sup>5</sup> Pure product was obtained as white solid in a yield of 40%. NMR matched with the literature values.

**R**-1-a: <sup>1</sup>H NMR (400 MHz, Chloroform-*d*):  $\delta$  2.46 (s, 1H), 2.22 (s, 1H), 1.98 (s, 1H), 1.89 (d,  $J$  = 3.2 Hz, 1H), 1.77 (m, 1H), 1.71 (m, 1H), 1.49 (m, 1H), 1.14 (m, 1H), 1.06 (s, 3H), 0.96 (s, 3H), 0.88 (s, 3H).

**S**-1-a: <sup>1</sup>H NMR (400 MHz, Chloroform-*d*):  $\delta$  2.50 (s, 1H), 2.27 (d,  $J$  = 13.4, 3.4 Hz, 1H), 2.01 (s, 1H), 1.94 (s, 1H), 1.81 (t,  $J$  = 4.2 Hz, 1H), 1.78 - 1.70 (m, 1H), 1.51 (dd,  $J$  = 26.7, 13.6, 4.5 Hz, 1H), 1.18 (dd,  $J$  = 14.9, 12.0 Hz, 1H), 1.10 (s, 3H), 1.00 (s, 4H), 0.92 (s, 3H).

Synthesis of (**R**)- and (**S**)-1-b: (**R**)-1-b and (**S**)-1-b were synthesized according to the literature procedure.<sup>6</sup> Au(tht)Cl (100 mg, 0.312 mmol) was dissolved in CH<sub>2</sub>Cl<sub>2</sub> (15 mL) and a solution of corresponding **R**- and **S**-1-a (71.26 mg, 0.4 mmol) in CH<sub>2</sub>Cl<sub>2</sub> (3 mL) was added in one portion followed by neat NEt<sub>3</sub> (5 drops, ca. 40 mg). The reaction mixture was stirred for 30 min in the absence of light. Yellow solution was filtered and evaporated. The solid was dissolved in CH<sub>2</sub>Cl<sub>2</sub>, washed with water (3  $\times$  15 mL), dried over Na<sub>2</sub>SO<sub>4</sub> in the absence of

light and evaporated. The resulting bright yellow residue was recrystallized to give bright yellow powder. The crude product was directly used in the next reaction without purification.

Synthesis of **1-d**: Au(tht)Cl (319.97 mg, 1.00 mmol) and phosphine ligand **1-c** (414.11 mg, 1.004 mmol) were dissolved in 15 mL CH<sub>2</sub>Cl<sub>2</sub> and stirred for 15 minutes. To the mixture was added dropwise an acetone solution (10 mL) of AgPF<sub>6</sub> (255.86 mg, 1.012 mmol). White precipitate was gradually formed and the suspension was stirred in the dark for 30 minutes. The mixture was filtered with suction through celite. The solution was purified by flash column chromatography. The obtained solid was dissolved in 5 ml acetone, and a large amount of ether was added to the solution. White solid was precipitated, filtered, washed with ether to obtain pure product. <sup>1</sup>H NMR (400 MHz, Chloroform-*d*): δ 7.66 - 7.57 (m, 16H), 7.55 - 7.46 (m, 24H), 3.48 (q, *J* = 7.0 Hz, 4H), 1.57 - 1.55 (m, 2H), 1.21 (t, *J* = 7.0 Hz, 6H). <sup>31</sup>P NMR (162 MHz, Chloroform-*d*): δ 41.04, -144.16.

Synthesis of (**R**)-**1** and (**S**)-**1**: (**R**)-**1** and (**S**)-**1** were synthesized according to the literature procedure.<sup>7</sup> **R-1-b** or **S-1-b** (93.5 mg, 0.025 mmol) was dissolved in a mixture solution of dichloromethane/acetone. **1-d** (93.5 mg, 0.062 mmol) was added in one portion. The reaction was stirred in the dark to give a yellow solution, which was filtered and evaporated, and the solid residue was recrystallized with CH<sub>2</sub>Cl<sub>2</sub>/ether. The yellow-green solid was obtained with a yield of 75% ((**R**)-**1**) and 78% ((**S**)-**1**), respectively.

(**R**)-**1**: <sup>1</sup>H NMR (400 MHz, Acetone-*d*<sub>6</sub>): δ 8.08 (dd, *J* = 12.9, 7.5 Hz, 8H), 7.88 (d, *J* = 19.7 Hz, 8H), 7.71 (t, *J* = 10.9 Hz, 8H), 7.64 - 7.59 (m, 8H), 7.55 - 7.46 (m, 8H), 4.93 (s, 4H), 4.01 (m, 3H), 3.39 (m, 5H), 3.16 (s, 1H), 2.57 (d, *J* = 12.9 Hz, 4H), 2.40 (m, 1H), 2.19 (m, 4H), 2.07 (m, 2H), 1.88 (d, *J* = 17.5 Hz, 8H), 1.69 (m, 5H), 1.60 (m, 5H), 1.23 (m, 6H), 1.16 (s, 12H), 1.03 (s, 12H), 0.91 (s, 12H). <sup>31</sup>P NMR (162 MHz, Acetone-*d*<sub>6</sub>): δ 15.42, -144.22. ESI-MS: *m/z*: 1/2[M-2PF<sub>6</sub>]<sup>2+</sup> calcd for C<sub>48</sub>H<sub>39</sub>AuN<sub>2</sub>P<sup>+</sup>: 1357.3065; found: 1357.9703.

(**S**)-**1**: <sup>1</sup>H NMR (400 MHz, Acetone-*d*<sub>6</sub>): δ 8.08 (dd, *J* = 12.7, 7.5 Hz, 8H), 7.90 - 7.84 (m, 8H), 7.74 - 7.67 (m, 8H), 7.64 - 7.59 (m, 8H), 7.54 - 7.46 (m, 8H), 4.92 (s, 4H), 4.02 (m, 3H), 3.39 (m, 5H), 3.15 (s, 2H), 2.57 (d, *J* = 12.8 Hz, 4H), 2.21 (s, 4H), 1.87 (d, *J* = 17.2 Hz, 9H), 1.75 - 1.65 (m, 5H), 1.65 - 1.54 (m, 5H), 1.22 (s, 6H), 1.16 (s, 12H), 1.03 (s, 12H), 0.91 (s, 12H). <sup>31</sup>P NMR (162 MHz, Acetone-*d*<sub>6</sub>): δ 15.43, -144.22. ESI-MS: *m/z*: 1/2[M-2PF<sub>6</sub>]<sup>2+</sup> calcd for C<sub>48</sub>H<sub>39</sub>AuN<sub>2</sub>P<sup>+</sup>: 1357.3065; found: 1357.9820.

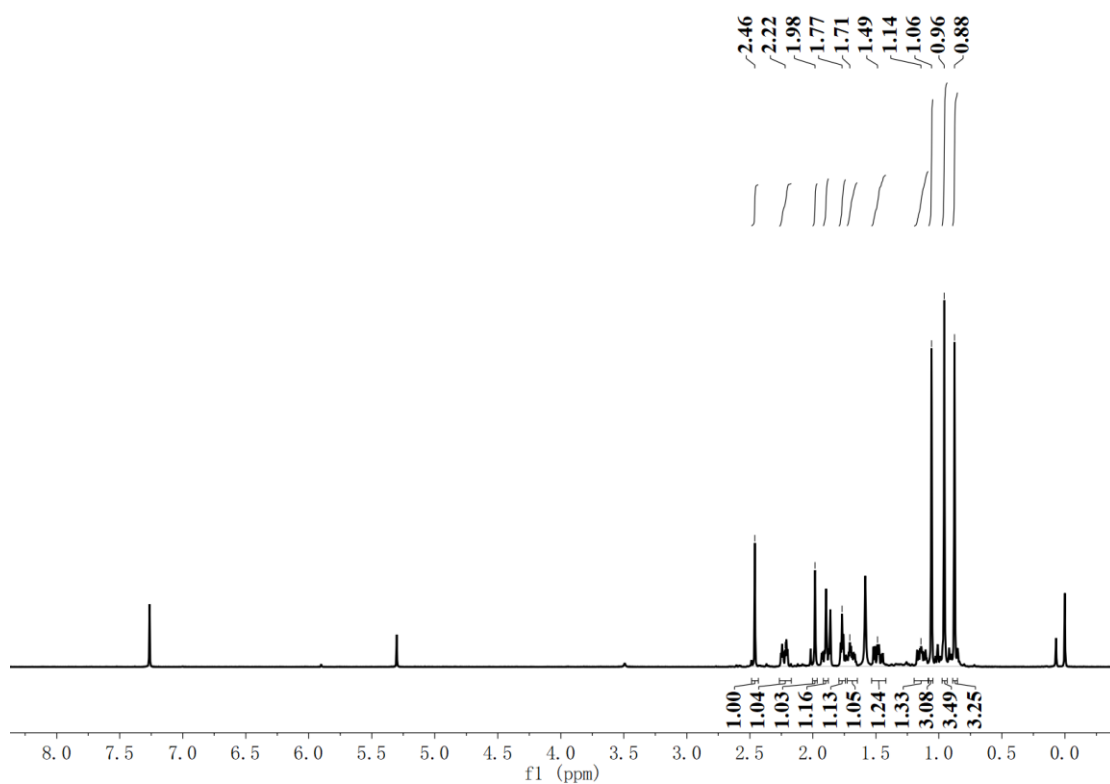


**Fig. S1**  $^1\text{H}$  NMR spectrum of (*R*)-**1-a** in  $\text{CDCl}_3$  at room temperature.

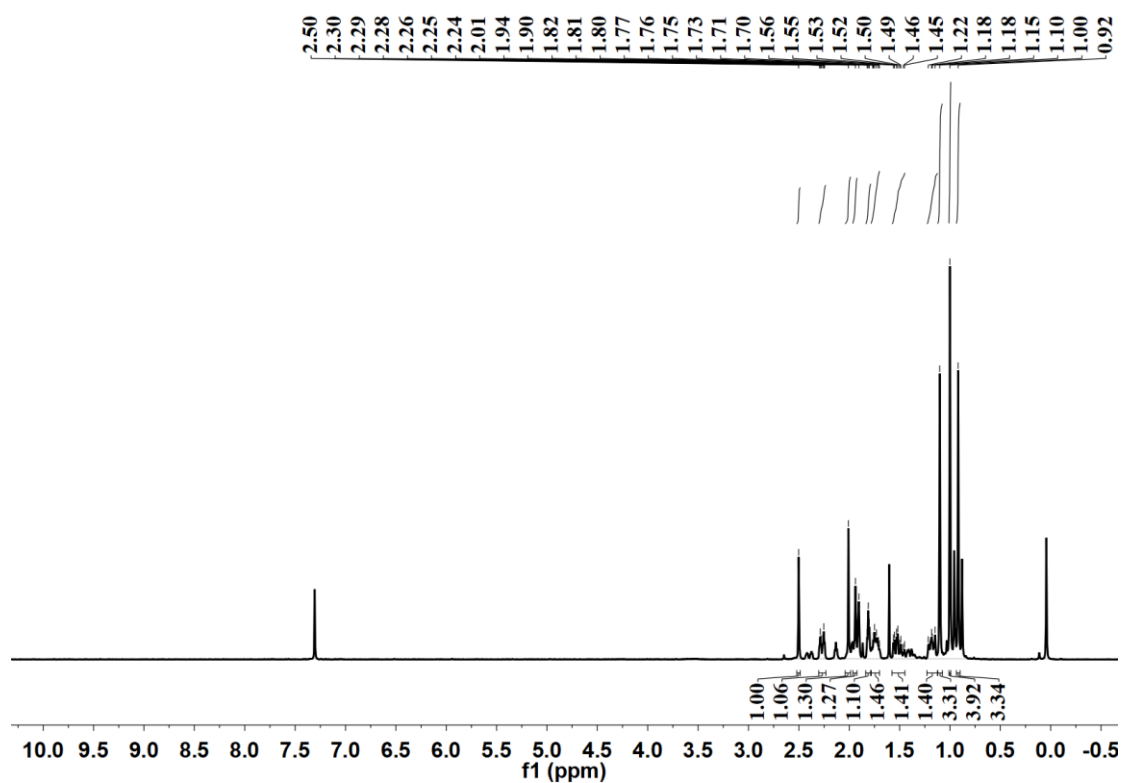


**Fig. S2**  $^1\text{H}$  NMR spectrum of (*S*)-**1-a** in  $\text{CDCl}_3$  at room temperature.

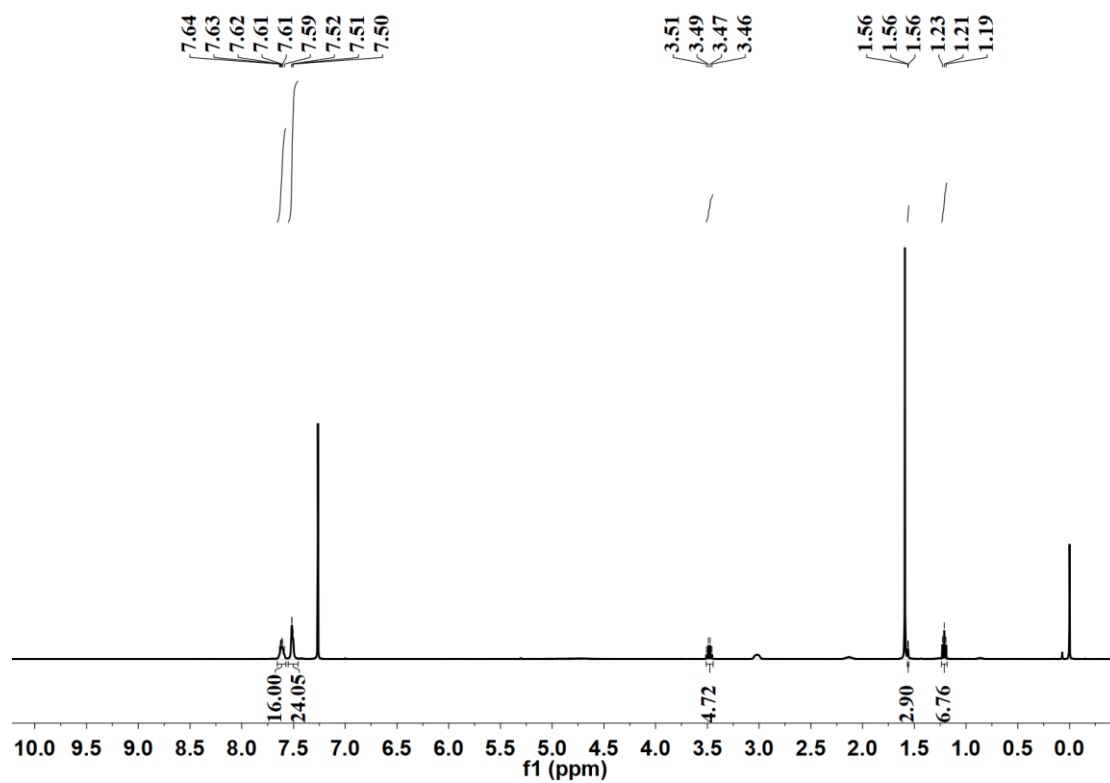


**Fig. S3**  $^1\text{H}$  NMR spectrum of **1-d** in  $\text{CDCl}_3$  at room temperature.

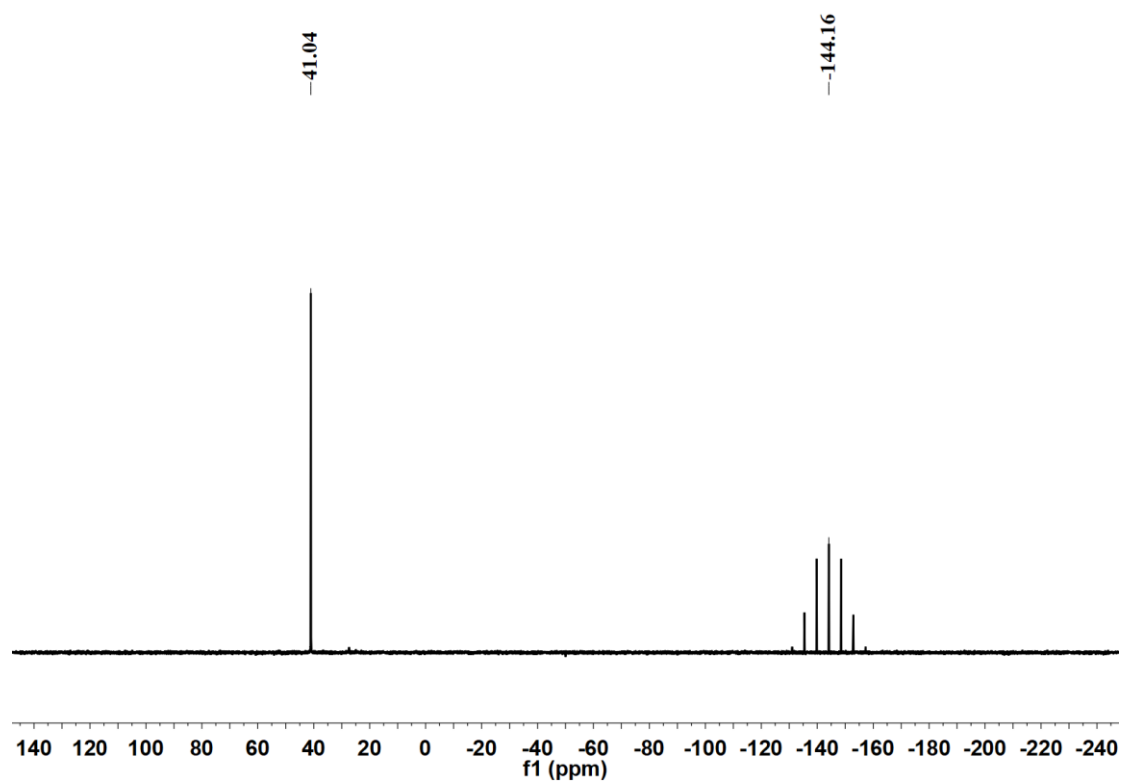


**Fig. S4**  $^{31}\text{P}$  NMR spectrum of **1-d** in  $\text{CDCl}_3$  at room temperature.

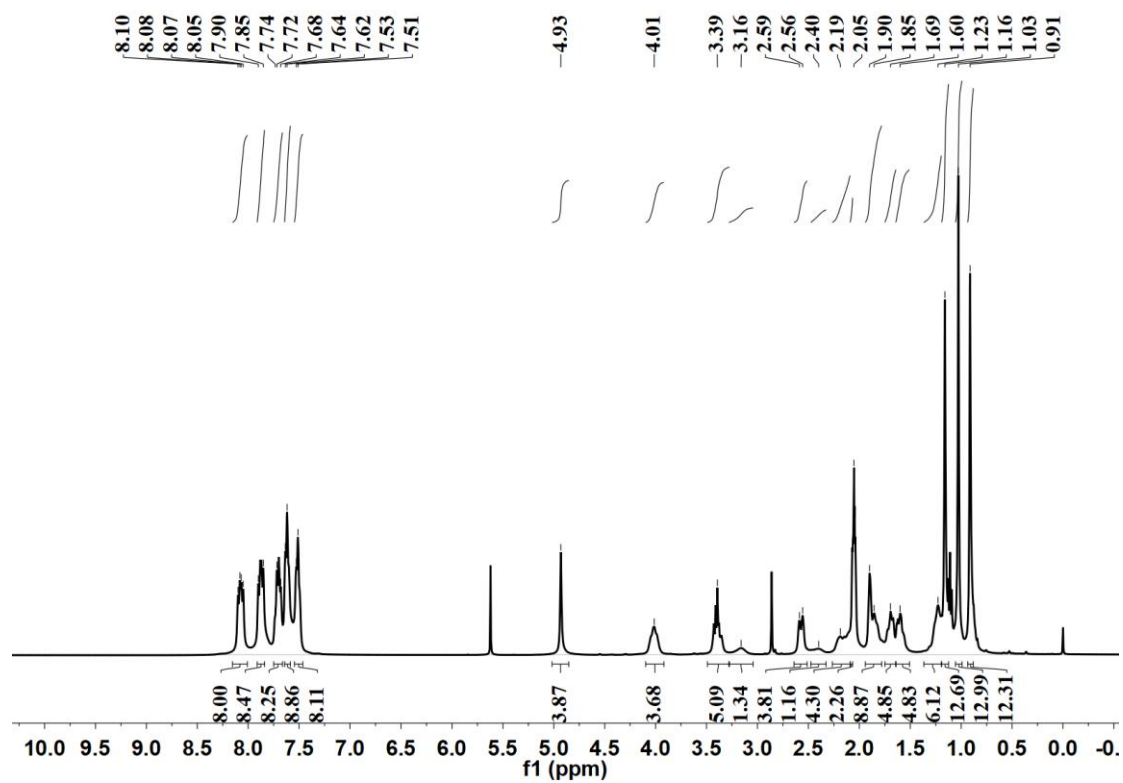


**Fig. S5**  $^1\text{H}$  NMR spectrum of (*R*)-**1** in acetone- $d_6$  at room temperature.

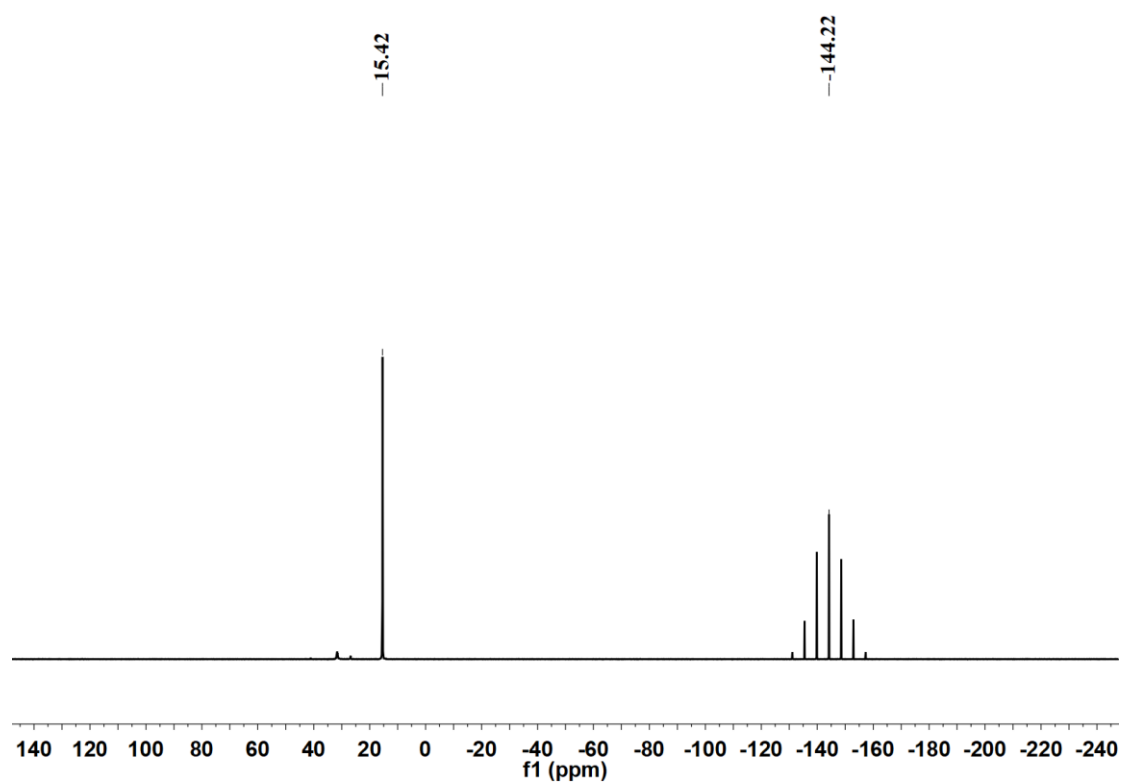


**Fig. S6**  $^{31}\text{P}$  NMR spectrum of (*R*)-**1** in acetone- $d_6$  at room temperature.

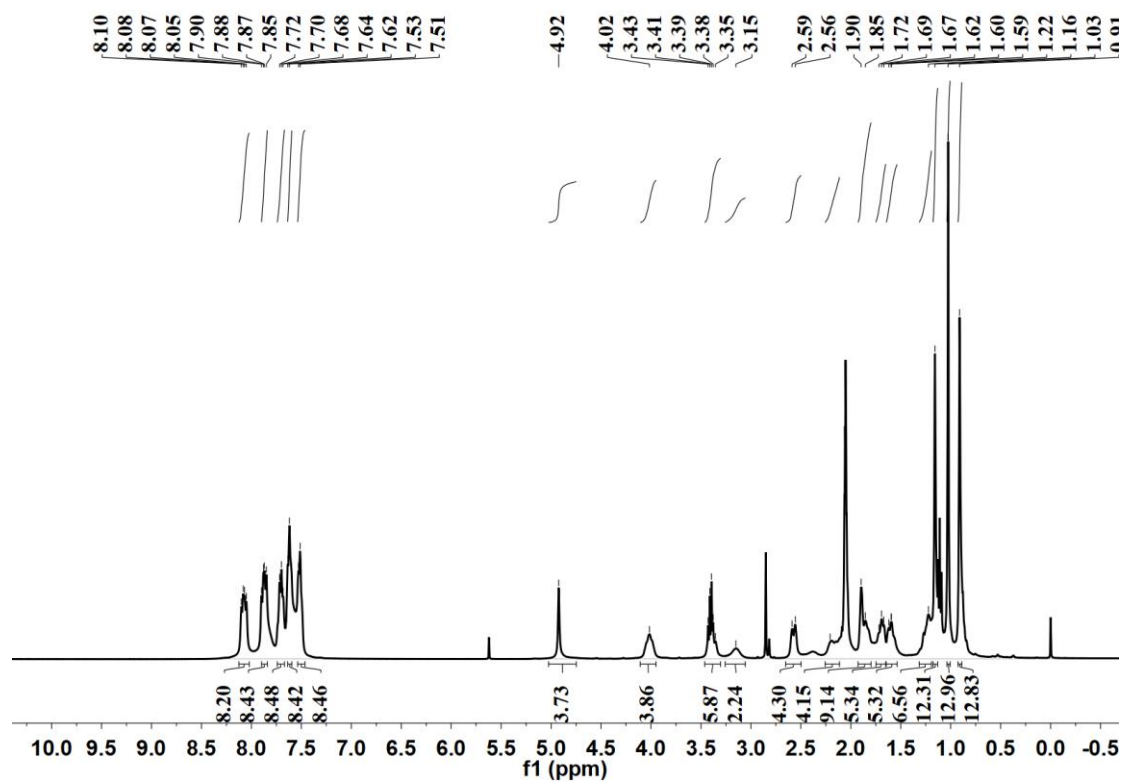


**Fig. S7**  $^1\text{H}$  NMR spectrum of (*S*)-**1** in acetone- $d_6$  at room temperature.

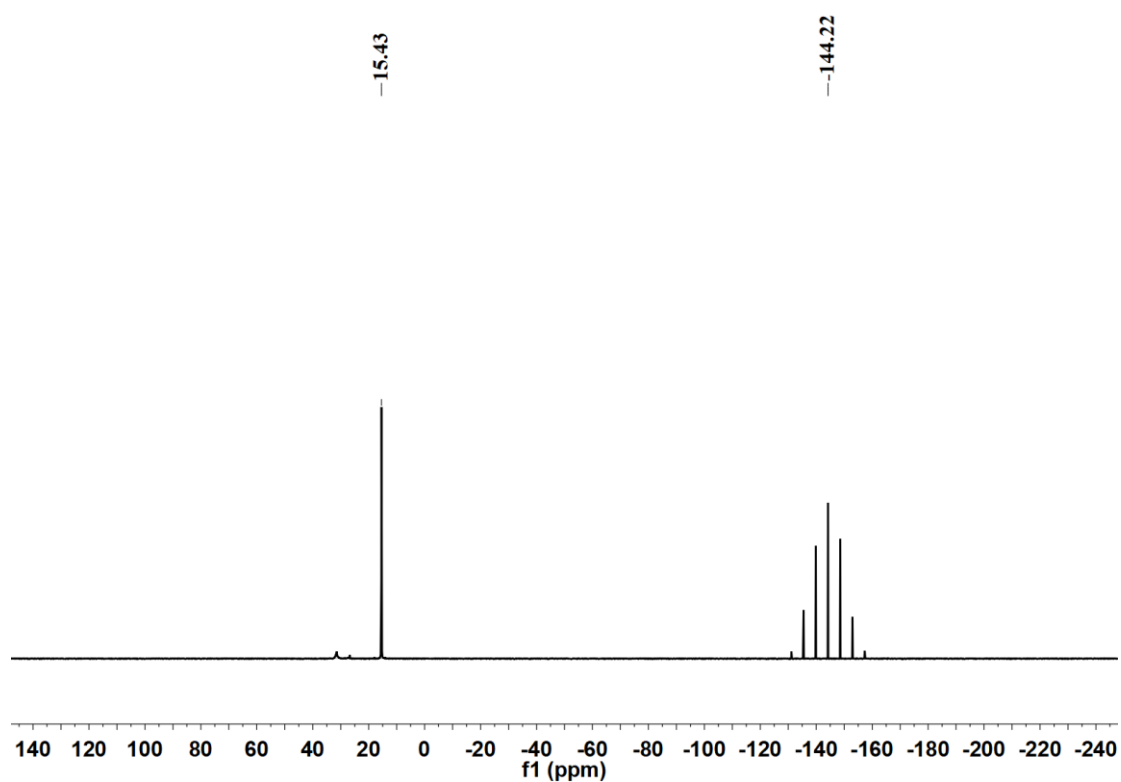


**Fig. S8**  $^{31}\text{P}$  NMR spectrum of (*S*)-**1** in acetone- $d_6$  at room temperature.

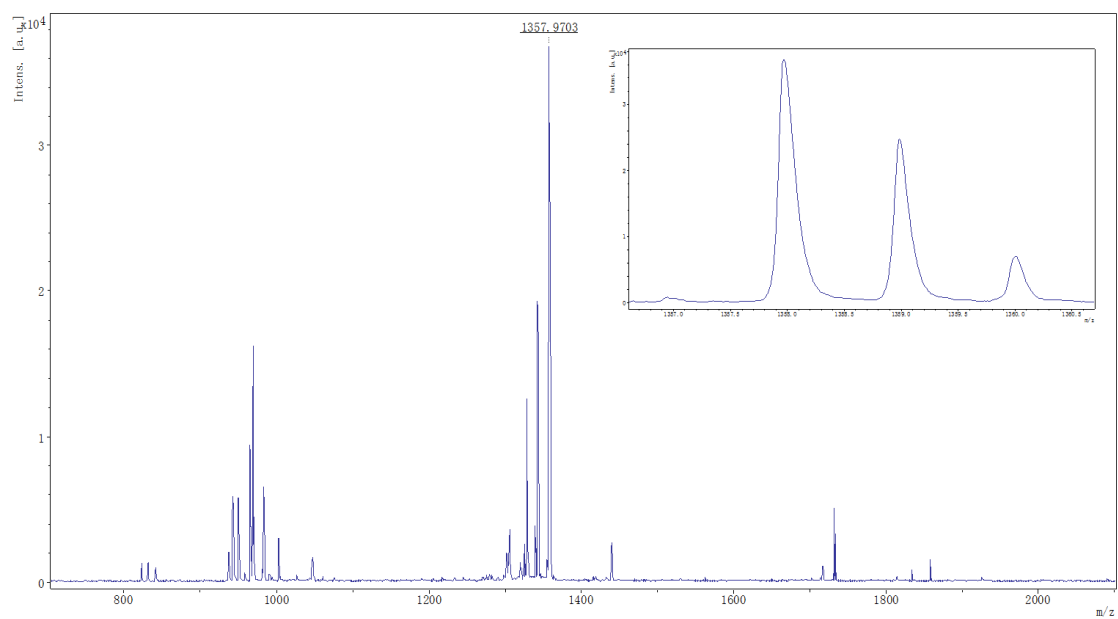


**Fig. S9** ESI-MS spectra of (*R*)-1.

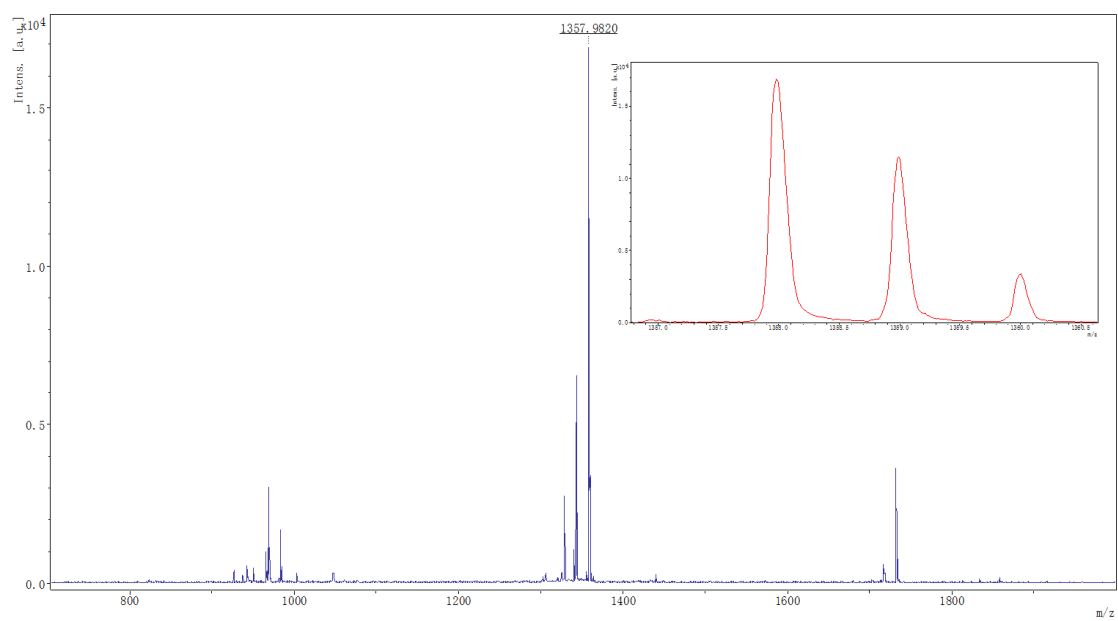


**Fig. S10** ESI-MS spectra of (*S*)-1.

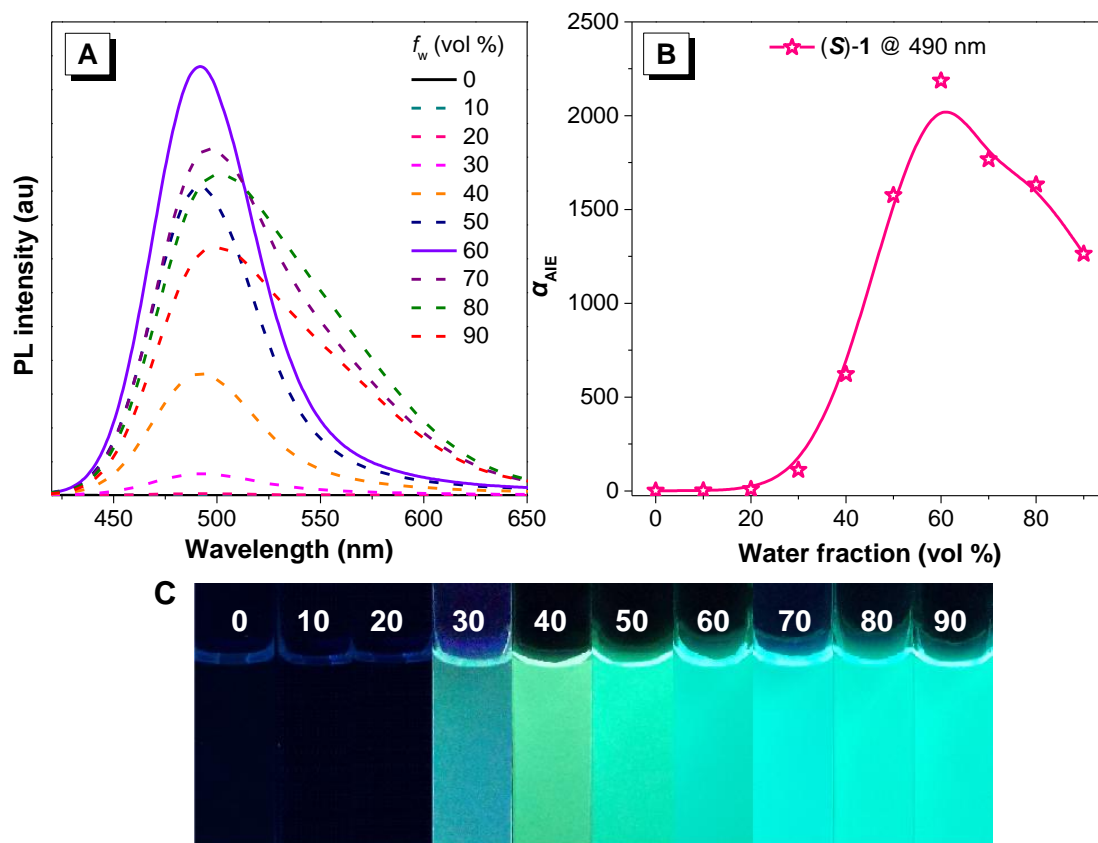


**Fig. S11** A) PL spectra of (*S*)-1 in DMF/water mixtures,  $\lambda_{\text{ex}} = 330$  nm. Concentration:  $5.0 \times 10^{-5}$  M. B) Plot of relative emission peak intensity ( $\alpha_{\text{AIE}}$ ) at 490 nm versus  $f_w$  of the DMF/water mixtures, where  $\alpha_{\text{AIE}} = I/I_0$ ,  $I$  = emission intensity and  $I_0$  = emission intensity in DMF solution. Inset: photos taken under 365 nm UV. C) Photos taken under 365 nm UV lamp.

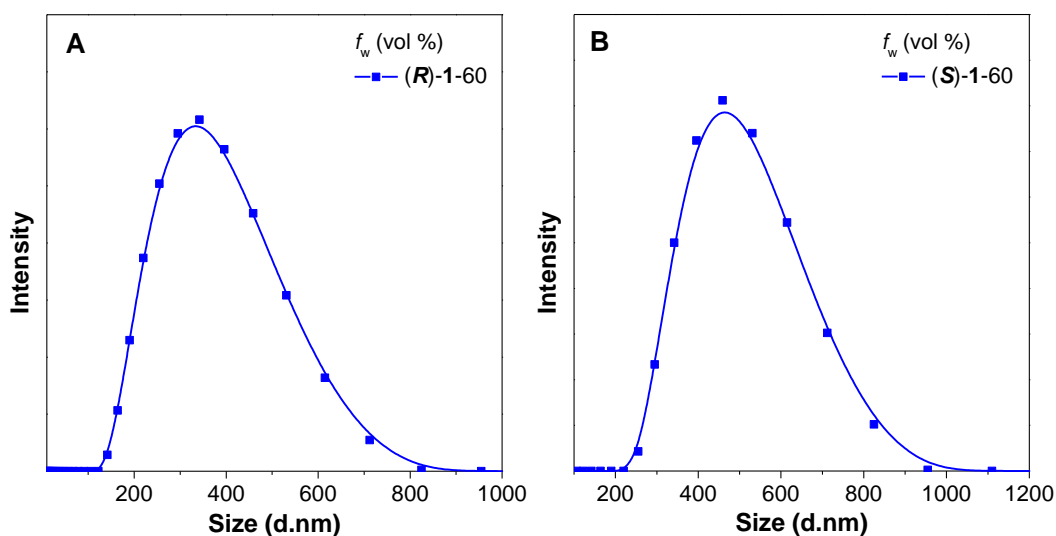


**Fig. S12** DLS spectra of (*R*)-1 (A) and (*S*)-1 (B) in DMF/water (2/3, v/v) mixtures.

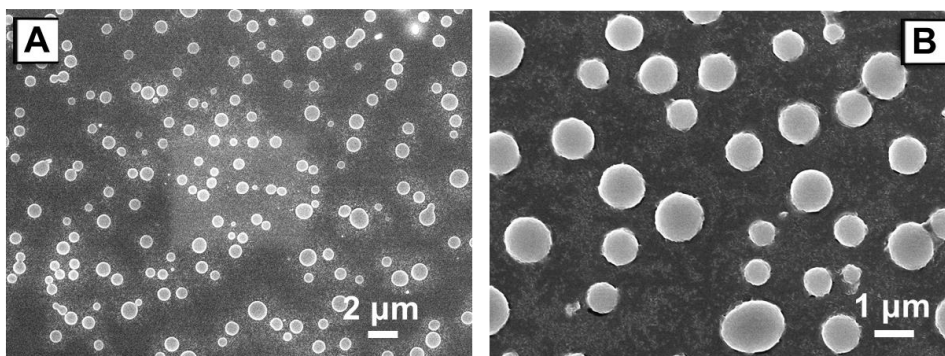


**Fig. S13** SEM images of (*S*)-1. Images were obtained from the evaporation of the fresh mixtures of DMF/water (2/3, v/v). Concentration:  $2 \times 10^{-5}$  M.

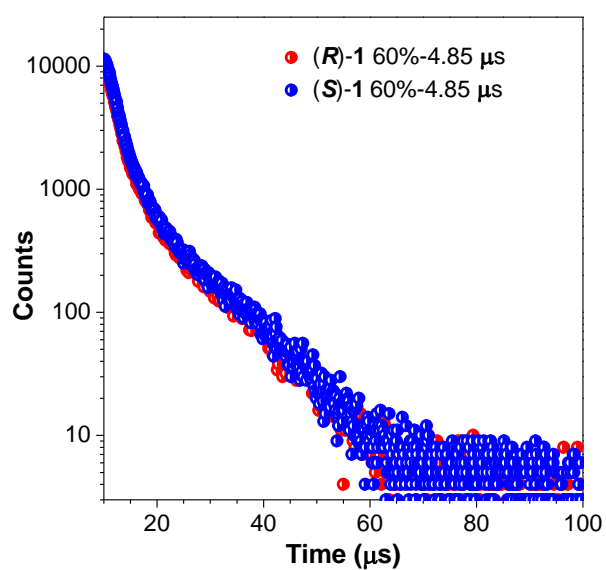


**Fig. S14** Lifetime of the DMF/water (2/3, v/v) mixtures of (*R*)-1 and (*S*)-1 at ambient temperature.

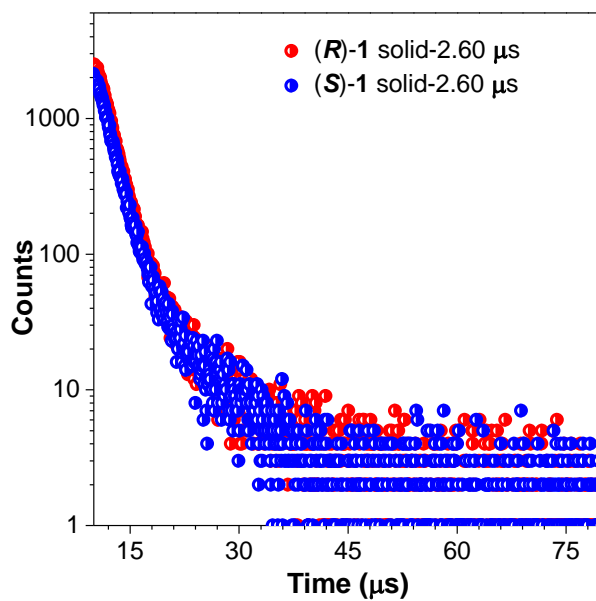


**Fig. S15** Lifetime of the crystalline powders of (*R*)-1 and (*S*)-1 at ambient temperature.

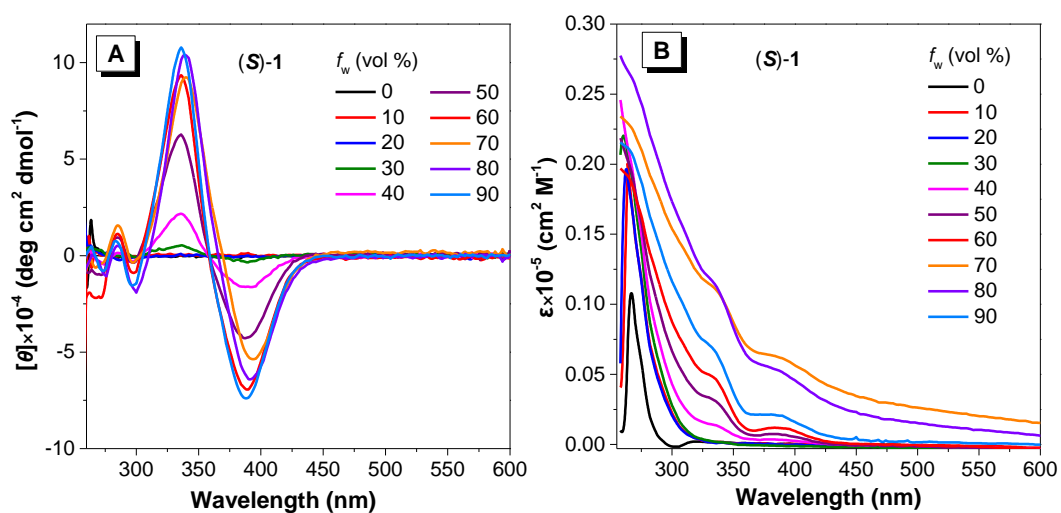


**Fig. S16** A) CD and B) UV spectra of (*S*)-1 measured in different DMF/water mixtures.

Concentration:  $5 \times 10^{-5}$  M.  $[\theta]$  = molar ellipticity.

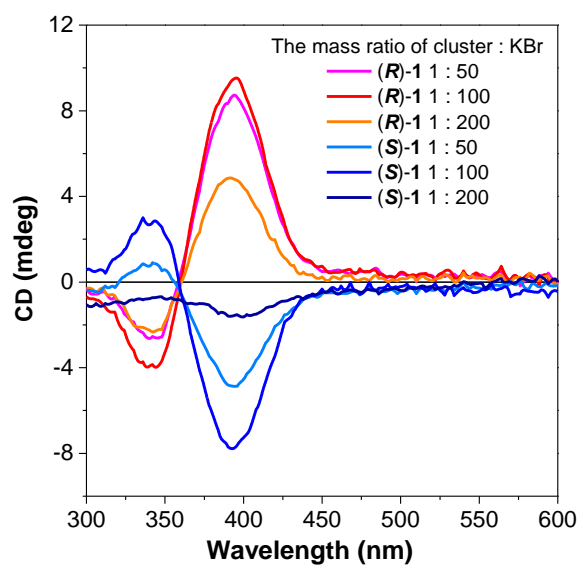


**Fig. S17** CD spectra of (*R*)-1 and (*S*)-1 in solid states.

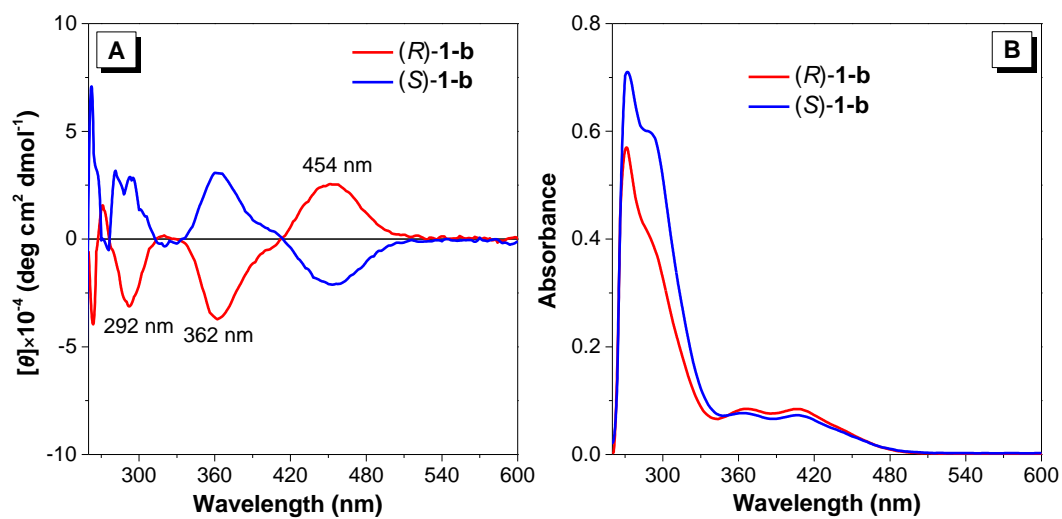


**Fig. S18** A) CD and B) UV spectra of (*R*)-1-b and (*S*)-1-b measured in the DMF/water (2/3),

v/v) mixtures. Concentration:  $5 \times 10^{-5}$  M.  $[\theta]$  = molar ellipticity.

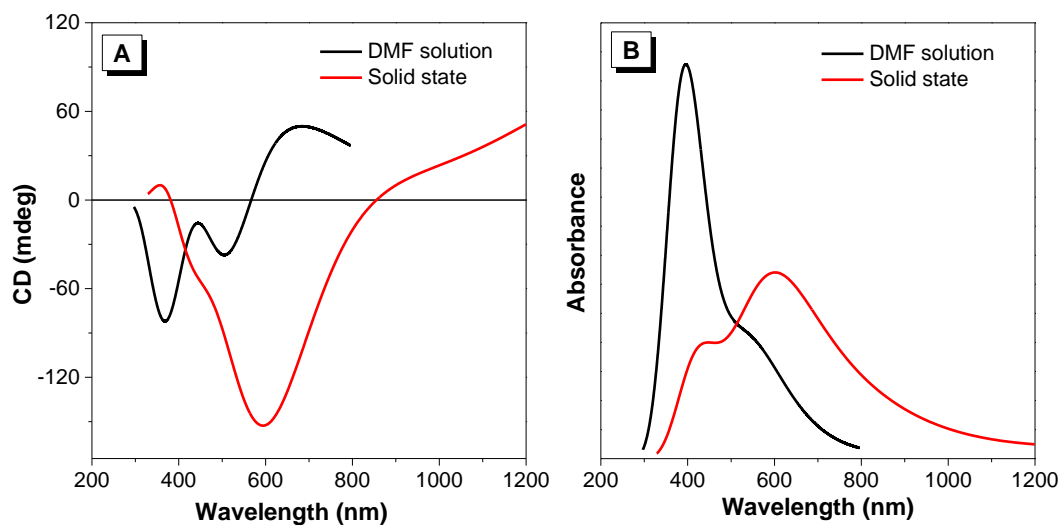


**Fig. S19** Simulated A) CD and B) UV spectra of (*S*)-1 in DMF solution and solid state, respectively.

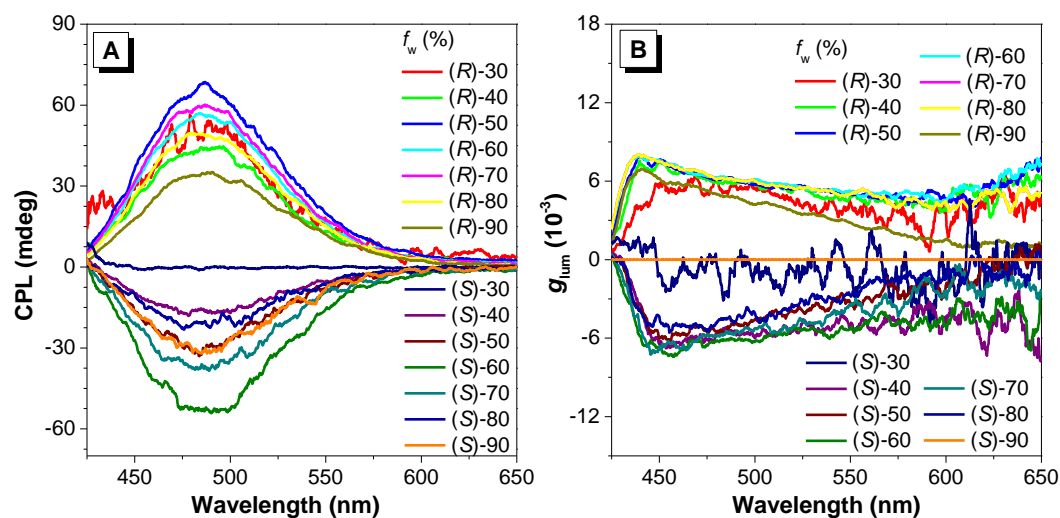


**Fig. S20** A) CPL spectra and B) corresponding dissymmetry factor  $g_{lum}$  of (*R*)-1 and (*S*)-1 in DMF/water mixtures. Concentration:  $5 \times 10^{-5}$  M.  $\lambda_{ex} = 340$  nm.

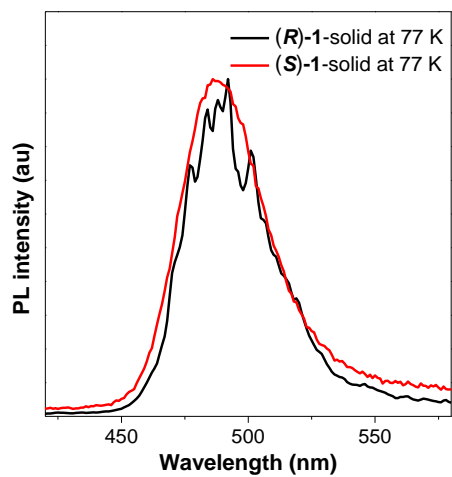


**Fig. S21** Phosphorescence spectra of crystalline powders of (*R*)-1 and (*S*)-1 at the low temperature (77 K).

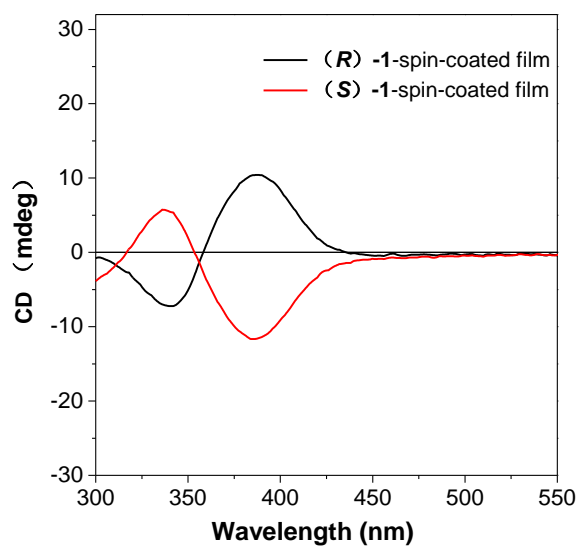


**Fig. S22** CD spectra of (*R*)-1 and (*S*)-1 in film.

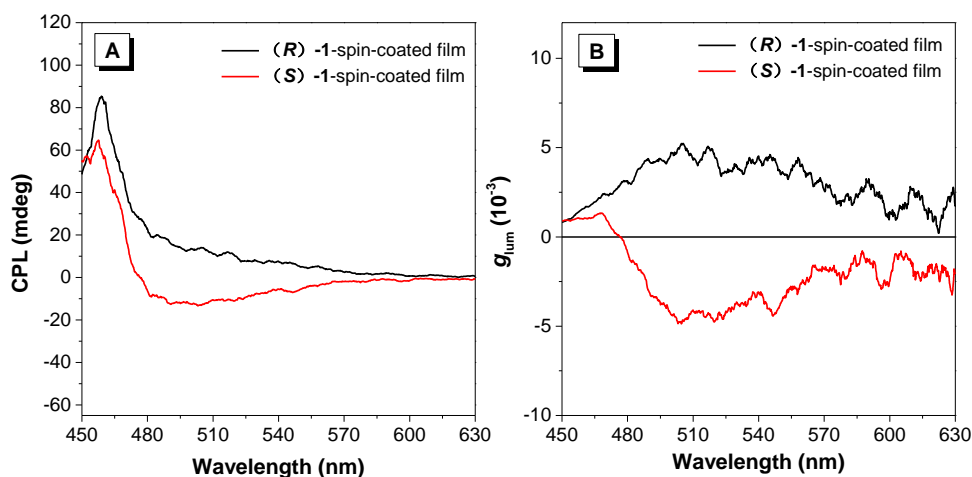


**Fig. S23** A) CPL spectra and B) corresponding dissymmetry factor  $g_{lum}$  of (*R*)-1 and (*S*)-1 in film.

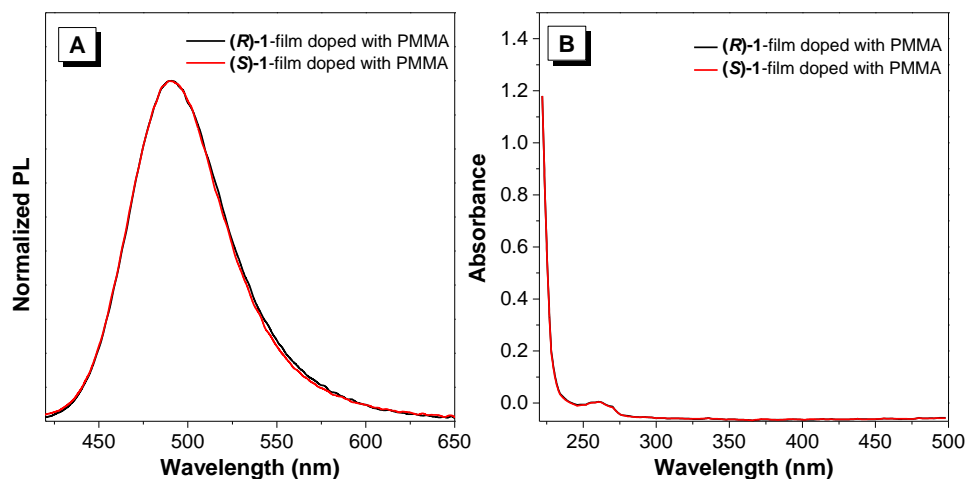


**Fig. S24** A) Normalized PL and B) absorption spectra of (*R*)-1 and (*S*)-1 in film doped with PMMA.

**Table S1** Crystal data and parameters of data collection and refinement for (*S*)-1.<sup>a</sup>

Complex	( <i>S</i> )-1
Empirical formula	$C_{102}H_{120}Au_6O_4P_4 \cdot 2(PF_6)$
Formula weight	3005.59
Temperature (K)	293
Crystal system	Orthorhombic
Space group	$C222_1$
$a$ (Å)	31.13 (4)
$b$ (Å)	14.257 (18)
$c$ (Å)	26.09 (3)

$\alpha$ (°)	90
$\beta$ (°)	90
$\gamma$ (°)	90
$V$ (Å <sup>3</sup> )	11579 (25)
$Z$	4
Density (calculated) (Mg/m <sup>3</sup> )	1.733
Absorption coefficient (mm <sup>-1</sup> )	7.72
$F(000)$	5744
Crystal size (mm <sup>3</sup> )	0.39 × 0.38 × 0.26
Theta range for data collection (°)	1.523 to 25.247
Index ranges	-37 ≤ $h$ ≤ 37, -17 ≤ $k$ ≤ 17, -31 ≤ $l$ ≤ 31
Reflections collected	32381
Independent reflections	10185 [ $R(\text{int}) = 0.139$ ]
Data / restraints / parameters	10185 / 264 / 557
Goodness-of-fit on $F^2$	1.03
Final $R$ indices [ $I > 2\sigma(I)$ ]	$R1 = 0.0846$ , $wR2 = 0.2003$
Final $R$ indices (all data)	$R1 = 0.1371$ , $wR2 = 0.2378$
Largest diff. peak and hole	3.45 and -3.08 e. <sup>-3</sup>

<sup>a</sup> Crystallographic data for the structure reported in this work has been deposited with the Cambridge Crystallographic Data Centre as supplementary publication no. CCDC: 1978728 for (S)-1.

## References

1. R. Uson, A. Laguna, M. Laguna, *Inorg. Synth.*, 1989, **26**, 85-91.
2. Gaussian 09, Revision D.01, Frisch, M. J.; Trucks, G. W.; Schlegel, H. B.; Scuseria, G. E.; Robb, M. A.; Cheeseman, J. R.; Scalmani, G.; Barone, V.; Mennucci, B.; Petersson, G. A.; Nakatsuji, H.; Caricato, M.; Li, X.; Hratchian, H. P.; Izmaylov, A. F.; Bloino, J.; Zheng, G.; Sonnenberg, J. L.; Hada, M.; Ehara, M.; Toyota, K.; Fukuda, R.; Hasegawa, J.; Ishida, M.; Nakajima, T.; Honda, Y.; Kitao, O.; Nakai, H.; Vreven, T.; Montgomery, J. A., Jr.; Peralta, J. E.; Ogliaro, F.; Bearpark, M.; Heyd, J. J.; Brothers, E.; Kudin, K. N.; Staroverov, V. N.; Kobayashi, R.; Normand, J.; Raghavachari, K.; Rendell, A.; Burant, J. C.; Iyengar, S. S.; Tomasi, J.; Cossi, M.; Rega, N.; Millam, J. M.; Klene, M.; Knox, J. E.; Cross, J. B.; Bakken, V.; Adamo, C.; Jaramillo, J.; Gomperts, R.; Stratmann, R. E.;

Yazyev, O.; Austin, A. J.; Cammi, R.; Pomelli, C.; Ochterski, J. W.; Martin, R. L.; Morokuma, K.; Zakrzewski, V. G.; Voth, G. A.; Salvador, P.; Dannenberg, J. J.; Dapprich, S.; Daniels, A. D.; Farkas, Ö.; Foresman, J. B.; Ortiz, J. V.; Cioslowski, J.; Fox, D. J. Gaussian, Inc., Wallingford CT, 2009.

3. T. Lu, F. Chen, *J. Comput. Chem.*, 2012, **33**, 580-592.
4. (a) M. Cossi, N. Rega, G. Scalmani, V. Barone, *J. Comput. Chem.*, 2003, **24**, 669-681; (b) V. Barone, M. Cossi, *J. Phys. Chem. A*, 1998, **102**, 1995-2001.
5. A. Singh, C. J. Fennella, J. D. Weaver. *Chem. Sci.*, 2016, **7**, 6796-6802.
6. I. O. Koshevoy, Y.-C. Chang, A. J. Karttunen, S. I. Selivanov, J. Jänis, M. Haukka, T. Pakkanen, S. P. Tunik, P.-T. Cho. *Inorg. Chem.*, 2012, **51**, 7392-7403.
7. I. O. Koshevoy, Y.-C. Chang, Y.-A. Chen, A. J. Karttunen, E. V. Grachova, S. P. Tunik, J. Janis, T. A. Pakkanen, P.-T. Chou. *Organometallics*, 2014, **33**, 2363-2371.